Available online at www.sciencedirect.com

SciVerse ScienceDirect

Ceramics International 39 (2013) 7391–7394

CERAMICS INTERNATIONAL

www.elsevier.com/locate/ceramint

# Microwave hydrothermal synthesis and optical properties of flower-like $Bi_2MoO_6$ crystallites

Ting Zhang, Jianfeng Huang*, Sen Zhou, Haibo Ouyang, Liyun Cao, Ating Li

*School of Materials Science and Engineering, Shaanxi University of Science and Technology, Xi'an, Shaanxi 710021, PR China*

Received 18 December 2012; received in revised form 23 February 2013; accepted 23 February 2013
Available online 1 March 2013

**Abstract**

Flower-like $Bi_2MoO_6$ crystallites were successfully synthesized by the microwave hydrothermal process using $Bi(NO_3)_3 \cdot 5H_2O$ and $Na_2MoO_4 \cdot 2H_2O$ as source materials and adding hexamethylene tetramine (HMT) as a template. X-ray diffraction (XRD) and field-emission scanning electron microscopy (FE-SEM) were used to characterize the products. Ultraviolet–visible (UV–vis) spectroscopy was employed to study the optical properties of $Bi_2MoO_6$. Results show that the product morphology is flower-like on adding the template. These flower-like $Bi_2MoO_6$ crystallites are a self-assembly of many thin nanoplates. HMT plays an important role in the formation of the flower-like morphology. UV–vis absorption spectra of all the $Bi_2MoO_6$ samples show strong photoabsorption properties from the ultraviolet region to the visible-light region with wavelength shorter than 500 nm. The band gap of flower-like $Bi_2MoO_6$ crystallites displays a slight red-shift compared with the $Bi_2MoO_6$ plate-like structures.


*Keywords:* Optical properties; Flower-like structure; $Bi_2MoO_6$

## 1. Introduction

It is well known that the morphology and size have extensive influence on the properties of materials. Therefore, many researchers have used capping agents, templates and/or surfactants in the chemical solution [1] to change the size of the inorganic compounds in recent years, because these changes could transform their functional properties such as optical, electrical and environmental ambience [2]. In the chemical synthesis, a variety of surfactants were employed to obtain new morphology and different sizes, which could promote the formation of materials with a large number of properties [3,4]. $Bi_2MoO_6$ is a typical Aurivillius-phase perovskite with a structure consisting of perovskite layers ($A_{m-1}B_mO_{3m+1}$) between bismuth oxide layers ($Bi_2O_2$) in bismuth oxide family [5–10]. $Bi_2MoO_6$ is interesting due to its unique physical properties of ion conduction [11], photoconductors [12] and gas sensors [13]. Moreover, it was also reported to be a visible-light responsive photocatalyst [14,15]. Various synthesis methods for this material have been reported. Among them are the molten salt method [16], organic precursor decomposition method [17], hydrothermal synthesis [18], etc. However, most of these methods need too long processing time and high temperature while the microwave hydrothermal process [19–21] permits synthesis of crystallites in shorter time and at lower temperature.

In this paper, flower-like $Bi_2MoO_6$ crystallites were successfully synthesized by the microwave hydrothermal process by adding hexamethylene tetramine (HMT) as the template. In addition, the optical properties of flower-like $Bi_2MoO_6$ crystallites have been investigated.

## 2. Experimental

### 2.1. Preparation

All of the chemicals were of analytical grade and used without further purification. In a typical synthesis, 2.5 mmol

*Corresponding author. Tel./fax: +86 29 86168802.
*E-mail addresses:* zhangt0205@163.com (T. Zhang), huangjfsust@126.com (J. Huang).

0272-8842/$ - see front matter © 2013 Elsevier Ltd and Techna Group S.r.l. All rights reserved.
http://dx.doi.org/10.1016/j.ceramint.2013.02.079

sodium molybdate ($Na_2MoO_4 \cdot 2H_2O$) and 5 mmol bismuth nitrate ($Bi(NO_3)_3 \cdot 5H_2O$) were dissolved in 25 mL of deionized water. 0.5 g hexamethylene tetramine (HMT) was added into the $Bi(NO_3)_3$ aqueous solution to form a homogeneous mixture under stirring. Then, the $Na_2MoO_4$ aqueous solution was added into the mixture slowly. After 20 min stirring, the mixture solution pH was adjusted to 3 with NaOH (10 mol/L). After 30 min stirring, the reaction solution was transferred into a 100 mL teflon-lined autoclave. The autoclave was put into a MDS-8 microwave hydrothermal system (Shanghai Sineo Microwave Chemistry Technology Co. Ltd., China). The system was set to the temperature-controlled mode to be maintained at 160 °C for 40 min. Subsequently, the autoclave was cooled to room temperature naturally. The product was collected and washed with distilled water and absolute ethanol several times. Finally, the product was dried in a drying cabinet at 80 °C for 5 h. A control experiment was also carried out without adding HMT while other experimental conditions were kept unchanged.

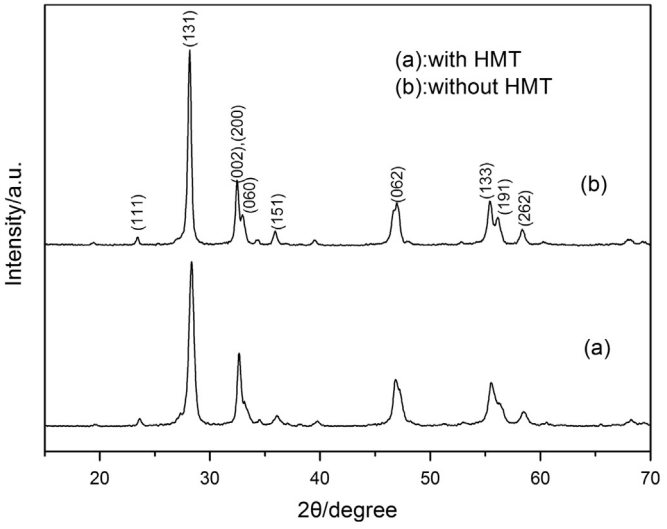


Fig. 1. X-ray diffraction patterns of $Bi_2MoO_6$ prepared by the microwave hydrothermal method (a) with and (b) without the addition of HMT.

### 2.2. Characterizations

The crystallite structure of the product was characterized by powder X-ray diffraction (XRD, D/MAX-2200PC, Rigaku, Japan) with CuKα radiation ($\lambda = 0.15406$ nm) at a scanning rate of $8^\circ\,min^{-1}$. The products morphologies were analyzed by a field-emission scanning electron microscope (FE-SEM, S-4800, Japan). The optical properties of the samples were obtained on an ultraviolet-visible spectrophotometer (UV–vis, Lambda 950, China).

## 3. Results and discussion

### 3.1. Crystallite structure

XRD patterns of $Bi_2MoO_6$ products synthesized by the microwave hydrothermal method with and without the addition of HMT are shown in Fig. 1. All of the peaks could be readily indexed to the phase of bismuth molybdate, with lattice constants of $a = 5.506$ Å, $b = 16.226$ Å, and $c = 5.487$ Å, which are in concordance with the standard JCPDS 72-1524 data of the $Bi_2MoO_6$ powder. No other impurities can be found. According to the XRD patterns, the intensity of some main diffraction peaks of $Bi_2MoO_6$ in Fig. 1(b), especially (131), becomes stronger and sharper compared with that in Fig. 1(a). The results indicate that the crystallinity of $Bi_2MoO_6$ prepared

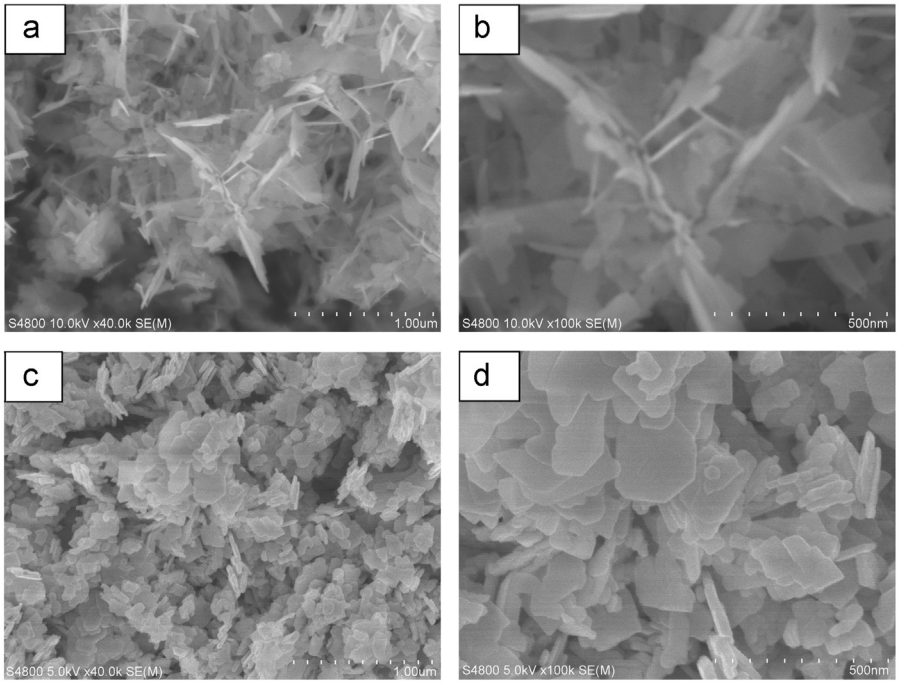


Fig. 2. FE-SEM images of $Bi_2MoO_6$ prepared by the microwave hydrothermal method (a), (b) with and (c), (d) without the addition of HMT.

without the addition of HMT is better than that of the product prepared with the addition of HMT.

### 3.2. Morphology

Fig. 2 presents the FE-SEM images of $Bi_2MoO_6$ prepared with and without the addition of HMT. The morphology of $Bi_2MoO_6$ crystallites prepared with HMT added as a template is flower-like (Fig. 2(a)). From the high-magnification FE-SEM images (Fig. 2(b)), the flower-like $Bi_2MoO_6$ crystallites are aggregates of many nanoplates. Compared with Fig. 2(c), these nanoplates are thinner, and irreversibly connect at their junctions to form a self-assembly architecture. Fig. 2(c) shows the FE-SEM image of plate-like $Bi_2MoO_6$ prepared in the absence of a template. The high-magnification FE-SEM image shown in Fig. 2(d) demonstrated that these plate-like structures were composed of many small nanoplates of a certain thickness on the basis of certain rules.

From Fig. 2, we can believe that HMT plays an important role in the morphology control to form flower-like $Bi_2MoO_6$. Once the crystalline phase is determined, the characteristic cell structures of the seeds strongly affect the further crystal growth [22]. As $Bi_2MoO_6$ has a layed perovskite structure, these morphologies in Fig. 2 are related to its own structure.

### 3.3. Optical properties

Fig. 3A displays the UV–vis absorption spectra of $Bi_2MoO_6$ with and without the addition of HMT. As can be seen, all the $Bi_2MoO_6$ samples show strong photoabsorption properties from ultraviolet region to visible-light region with the wavelength shorter than 500 nm. They both have steep shape of the absorption edge, which indicates a band-gap transition rather than the transition from the impurity levels [23]. Therefore, $Bi_2MoO_6$ has great potential applications in the fields of visible-light photocatalysis and photoluminescence. As $Bi_2MoO_6$ is a direct band gap semiconductor, according to the equation $(\alpha hv)^2 = A(hv - E_g)$, where $\alpha$, $h$, $v$, $E_g$, and $A$ are absorption coefficient, Planck constant, light frequency, band gap, and a constant, respectively. The band gaps of flower-like and plate-like $Bi_2MoO_6$ can be estimated to be about 2.76 eV and 2.62 eV, respectively, as shown in Fig. 3B. From this we can observe a slight red-shift of the absorption band edge of the $Bi_2MoO_6$ samples. It is well known that the band gap energy of semiconductor nanoparticles increases with the decrease of grain size. Therefore, flower-like $Bi_2MoO_6$ crystallites display a slight red-shift of the absorption band edge compared with the plate-like structured $Bi_2MoO_6$, due to the smaller grain sizes of the flower-like $Bi_2MoO_6$ crystallites than those of the plate-like structured $Bi_2MoO_6$ as shown in Fig. 1.

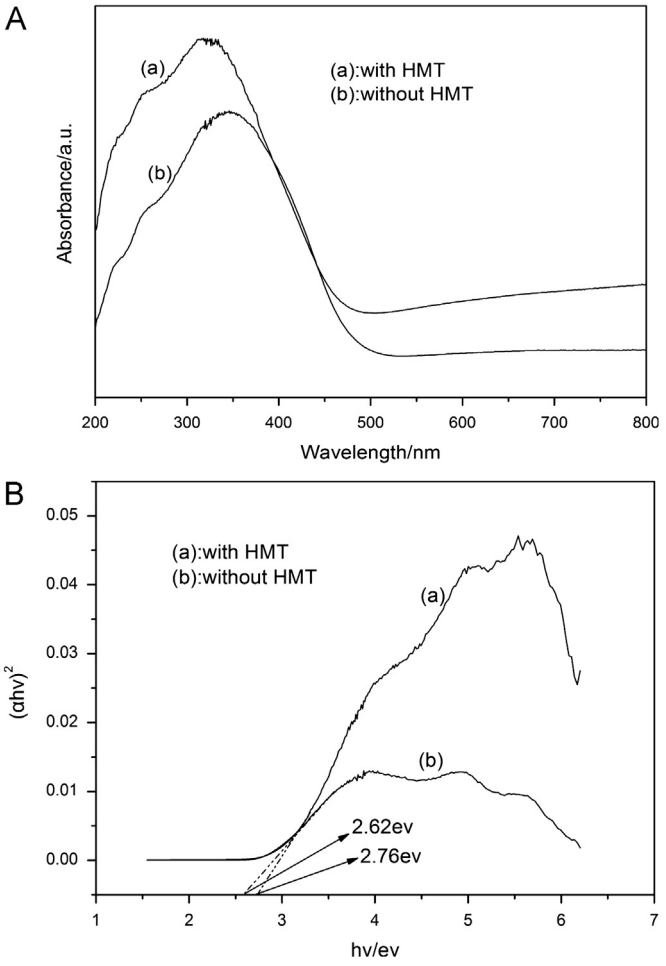


Fig. 3. UV–vis absorption spectra (A) and plots of the $(\alpha hv)^2$ vs photon energy ($hv$) (B) of $Bi_2MoO_6$ synthesized by the microwave hydrothermal method (a) with and (b) without the addition of HMT.

## 4. Conclusions

$Bi_2MoO_6$ crystallites with a flower-like structure consisting of nanoplates have been synthesized by the microwave hydrothermal method by adding HMT as a template at 160 °C for 40 min. UV–vis absorption spectra results indicate that all the $Bi_2MoO_6$ samples have strong photoabsorption properties from ultraviolet region to visible-light region with the wavelength shorter than 500 nm. And the absorption band edge of flower-like $Bi_2MoO_6$ crystallites displays a slight red-shift compared with that of the $Bi_2MoO_6$ plate-like structures.

## Acknowledgments

This work was financially supported by the National Science Foundation of China (50942047), Natural Science Foundation of Shaanxi Province of China (2010JM, 2010JM6017), International Science and Technology Cooperation Project of Shaani Province (2011KW-110) and the Graduate Innovation Foundation of Shaanxi University of Science and Technology.

## References


[1] C. Burda, X. Chen, R. Narayanan, M.A. El-Sayed, Chemistry and properties of nanocrystals of different shapes, Chemical Reviews 105 (2005) 1025–1102.

[2] Z. Nie, A. Petukhova, E. Kumacheva, Properties and emerging applications of self-assembled structures made from inorganic nanoparticles, Nature Nanotechnology 15 (2010) 15–25.

[3] H. Shi, L. Qi, J. Ma, H. Cheng, Polymer-directed synthesis of penniform $BaWO_4$ nanostructures in reverse micelles, Journal of the American Chemical Society 125 (2003) 3450–3451.

[4] F. Lei, B. Yan, H.H. Chen, Q. Zhang, J.T. Zhao, Surfactant-assisted hydrothermal synthesis, physical characterization, and photoluminescence of $PbWO_4$, Crystal Growth and Design 9 (2009) 3730–3736.

[5] R.E. Newnmam, R.W. Wolfe, J.F. Dorrian, Structural basis of ferroelectricity in the bismuth titanate family, Materials Ressearch Bulletin 6 (1971) 1029–1039.

[6] J.L. Hutchison, J.S. Anderson, C.N.R. Rao, Electron microscopy of ferroelectric bismuth oxides containing perovskite layers, Proceedings the Royal of Society A 355 (1977) 301–312.

[7] Y. Bando, A. Watanabe, Y. Sekikawa, M. Goto, S. Horiuchi, New layered structure of $Bi_2W_2O_9$ determined by 1 MV high-resolution electron microscopy, Acta Crystallographica Section A 35 (1979) 142–145.

[8] B. Frit, J.P. Mercorio., The crystal chemistry and dielectric properties of the Aurivillius family of complex bismuth oxides with perovskite-like layered structures, Journal of Alloys and Compounds 188 (1992) 27–35.

[9] M.T. Montero, P. Millan, P. Duran-Martin, B. Jimenez, A. Catro, Solid solutions of lead-doped bismuth layer of Aurivillius $n=2$ and $n=3$ oxides: structural and dielectric characterization, Materials Research Bulletin 33 (1998) 1103–1115.

[10] A. Watanabe, M. Goto, Characterization of $Bi_2W_2O_9$ having a unique layered structure, Journal of the Less Common Metals 61 (1978) 265–272.

[11] L.T. Sim, C.K. Lee, A.R. West, High oxide ion conductivity in $Bi_2MoO_6$ oxidation catalyst, Journal of Materials Chemistry 12 (2002) 17–19.

[12] T. Sekiya, A. Tsuzuki, Y. Torii, Elaboration et photoconduction des films de $Bi_2O_3$–$MO_3$ (M=Mo OU W) obtenus par hypertrempe, Materials Research Bulletin 21 (1986) 601–608.

[13] N. Hykaway, W.M. Sears, R.F. Frindt, S.R. Morrison., The gas-sensing properties of bismuth molybdate evaporated films, Sensors and Actuators 15 (1988) 105–118.

[14] A. Kudo, S. Hijii, $H_2$ or $O_2$ evolution from aqueous solutions on layered oxide photocatalysts consisting of $Bi^{3+}$ with $6s^2$ configuration and $d^0$ transition metal ions, Chemistry Letters (1999) 1103–1104.

[15] H. Kato, M. Hori, R. Konta, Y. Shimodaira, A. Kudo, Construction of Z-scheme type heterogeneous photocatalysis systems for water splitting into $H_2$ and $O_2$ under visible light irradiation, Chemistry Letters 33 (2004) 1348–1349.

[16] L. Xie, J. Ma, G. Xu, Preparation of a novel $Bi_2MoO_6$ flake-like nanophotocatalyst by molten salt method and evaluation for photocatalytic decomposition of Rhodamine B, Materials Chemistry and Physics 110 (2008) 197–200.

[17] A. Cruz, S.O. Alfaro, E.L. Cudllar, U.O. Mdndez, Photocatalytic properties of $Bi_2MoO_6$ nanoparticles prepared by an amorphous complex precursor, Catalysis Today 129 (2007) 194–199.

[18] H.H. Li, K.W. Li, H. Wang, Hydrothermal synthesis and visible-light photocatalytic properties of $\alpha$-$Bi_2Mo_3O_{12}$ and $\gamma$-$Bi_2MoO_6$, Chinese Journal of Inorganic Chemistry 25 (2009) 512–516.

[19] Z.Q. Li, X.T. Chen, Z.L. Xue, Microwave-assisted synthesis and photocatalytic properties of flower-like $Bi_2WO_6$ and $Bi_2O_3$–$Bi_2WO_6$ composite, Journal of Colloid and Interface Science 394 (2013) 69–77.

[20] H.D. Xie, D.Z. Shen, X.Q. Wang, G.Q. Shen, Microwave hydrothermal synthesis and visible-light photocatalytic activity of $\gamma$- $Bi_2MoO_6$ nanoplates, Materials Chemistry and Physics 110 (2008) 332–336.

[21] H.D. Xie, D.Z. Shen, X.Q. Wang, G.Q. Shen, Microwave hydrothermal synthesis and visible-light photocatalytic activity of $Bi_2WO_6$ nanoplates, Materials Chemistry and Physics 103 (2007) 334–339.

[22] Y.W. Jun, J.S. Choi, J. Cheon, Shape control of semiconductor and metal oxide nanocrystals through nonhydrolytic colloidal routes, Angewandte Chemie, International Edition 45 (2006) 3414–3439.

[23] L. Zhou, W.Z. Wang, L.S. Zhang, Ultrasonic-assisted synthesis of visible-light-induced $Bi_2MO_6$ (M=W, Mo) photocatalysts, Journal of Molecular Catalysis A: Chemical 268 (2007) 195–200.